WFL: Microwave Applications of Thin Ferroelectric Films

Robert Romanofsky

NASA Glenn Research Center

Antenna and Optical Systems Branch

Cleveland OH

Outline:

- Introduction
- A Statistical Analysis of Ferroelectric Film Quality
- Phase Shifters
- Oscillators
- The Reflectarray Antenna
- Radiation Testing
- Ferroelectric Reflectarray Critical Components Space Experiment
- A Piezoelectric Transformer Driver for Ferroelectric Devices
- An Agile Microstrip Patch Antenna
- “Strange” Results
  - 1/f noise
  - Anomalous Magnetoresisteiove Effect

Crystal Structure of Displacement Type Ferroelectrics

(a) Crystal lattice cell of $BaTiO_3$

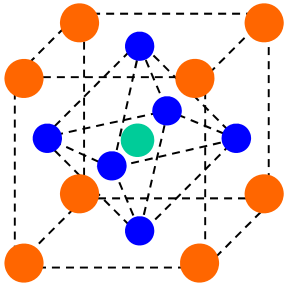

O

Ti

Ba

(a) Oxygen sublattice

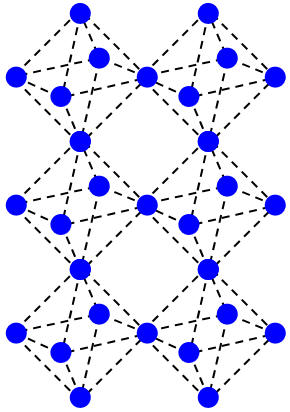

(b) Titanium sublattice

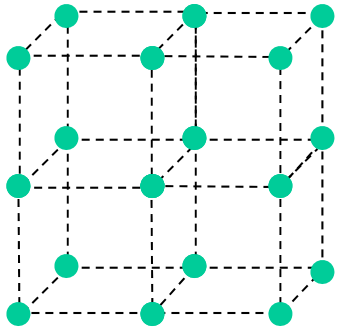

(b) Deformation of the cell followed by the polarization

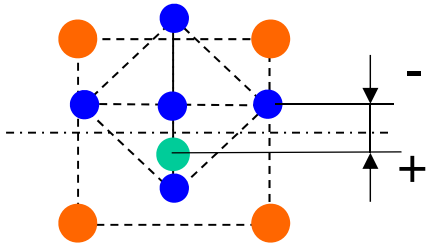

Dipole

Mutual displacement of Ti and O sublatticies is followed by formation of an electric dipole and polarization of the crystal

where q is the charge, x is displacement, V_c is volume of the crystal cell

$$P = \frac{q \cdot x}{V_c}$$

Ferroelectric Technology: Films to Devices to a Space Experiment

Modified 615 Element Scanning Ferroelectric Reflectarray: 2005-2009
Prototype antenna with practical low-power controller assembled and installed in NASA GRC far-field range for testing. Low-cost, high-efficiency alternative to conventional phased arrays

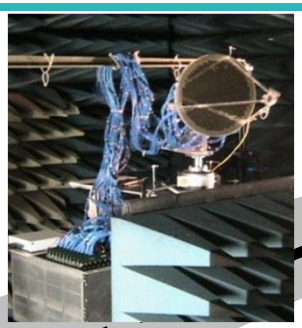

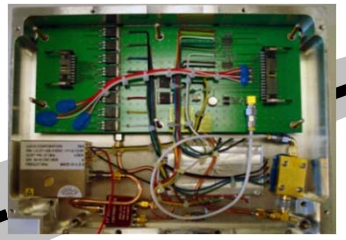

MISSE-8 Space Experiment: 2010
Launched STS-134 includes 8 active $Ba_xSr_{1-x}TiO$ Ka-band phase shifters

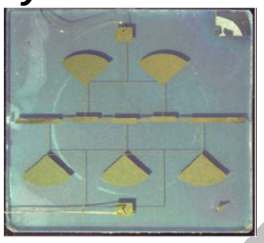

Thin film ferroelectric phase shifter on Magnesium Oxide

Cellular Reflectarray: 2010 Derivative attracts attention for commercial next generation DirecTV, etc. applications

Practical Phase Shifters : 2003-2004 ***Novel phased array concept based on quasi-optical feed and low-loss ferroelectric phase shifters refined. 50 wafers of Ba0.5Sr0.5TiO3 on lanthanum aluminate processed to yield over 1000 ferroelectric K-band phase shifters. Radiation tests show devices inherently rad hard in addition to other advantages over GaAs***

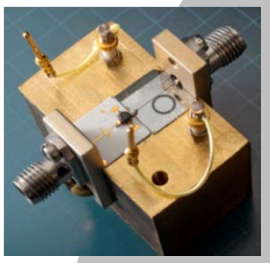

First Ku-Band tunable Oscillator based on thin ferroelectric films

Fundamental Research: 2000-2003 ***Agile microwave circuits are developed [using room temperature Barium Strontium Titanate ($Ba_{0.5}Sr_{0.5}TiO_3$)], including oscillators, filters, antenna elements, etc., that rival or even outperform their semiconductor counterparts at frequencies up to Ka-band***

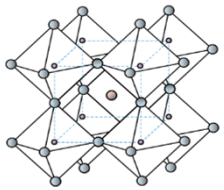

Parent crystal: Strontium Titanate

Seedling Idea: 1997-1999 ***Basic experiments with strontium titanate at cryogenic temperatures suggest loss tangent of ferroelectric films may be manageable for microwave applications***

Statistical Analysis of 48 PLD $Ba_{50}Sr_{50}TiO_3$ Films on $LaAlO_3$

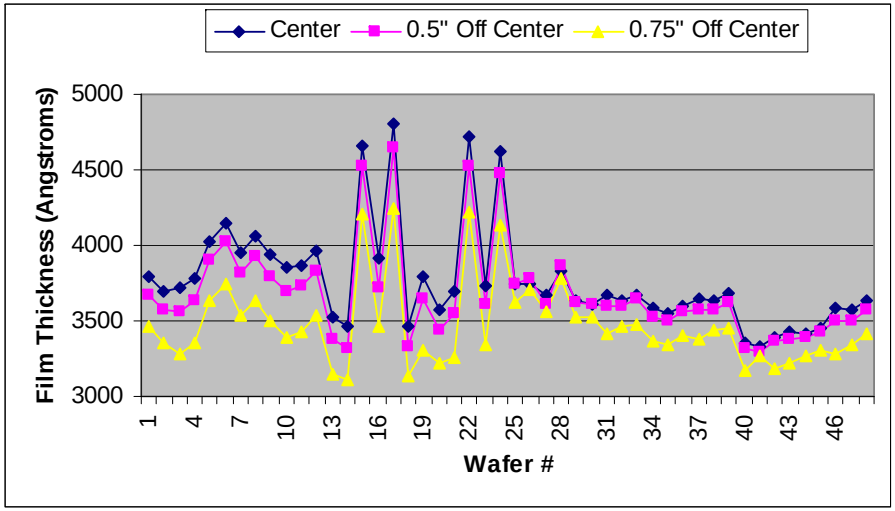

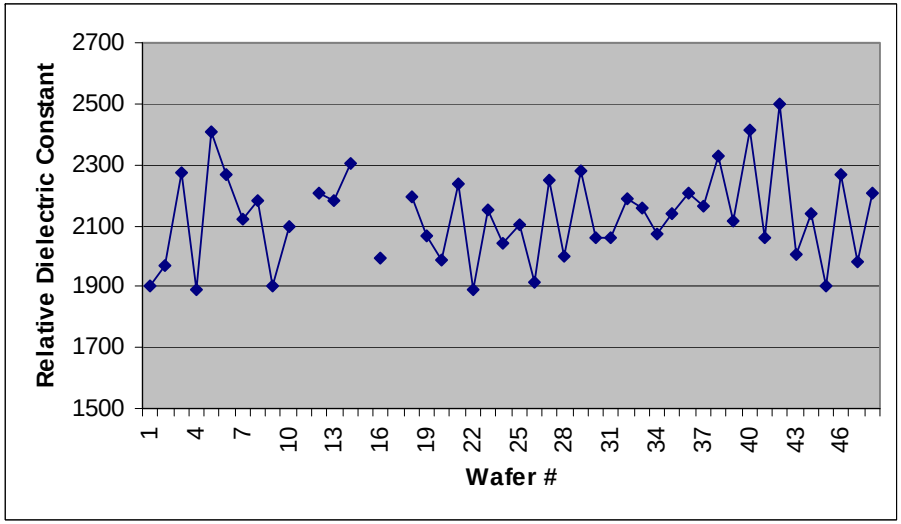

Peak (0 Field) Dielectric Constant Variation From Wafer to Wafer

- 48 BSTO (50:50)/$LaAlO_3$ wafers from Neocera, Inc. were RF characterized using a novel on-wafer probe technique and compared to high resolution XRD and ellipsometric data

- The performance uniformity in terms of Q, phase shift and peak dielectric constant was excellent. Q=14.1,σ =1.0; ε=2129, σ=149, Average phase/ element=20.5º, σ =1.4º.

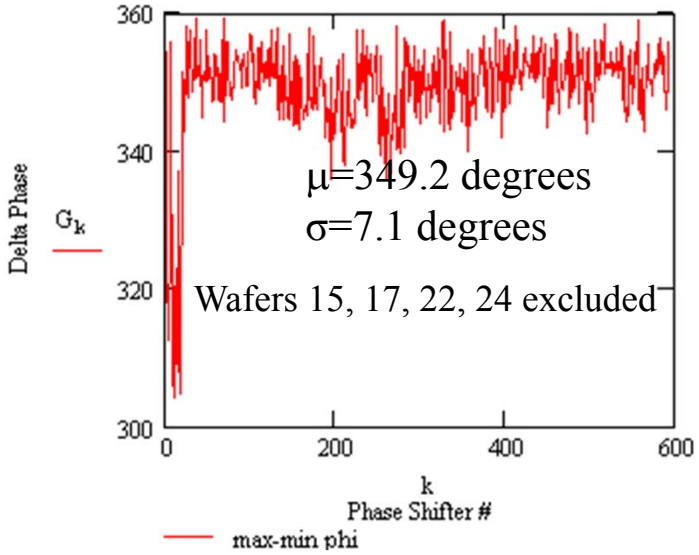

Romanofsky et al., Mat. Res. Soc. Proc. Vol. 603, pp 3-14, 2000

Summary of full width, half maximum measurements of the (002) BST peak, for films deposited at different times.

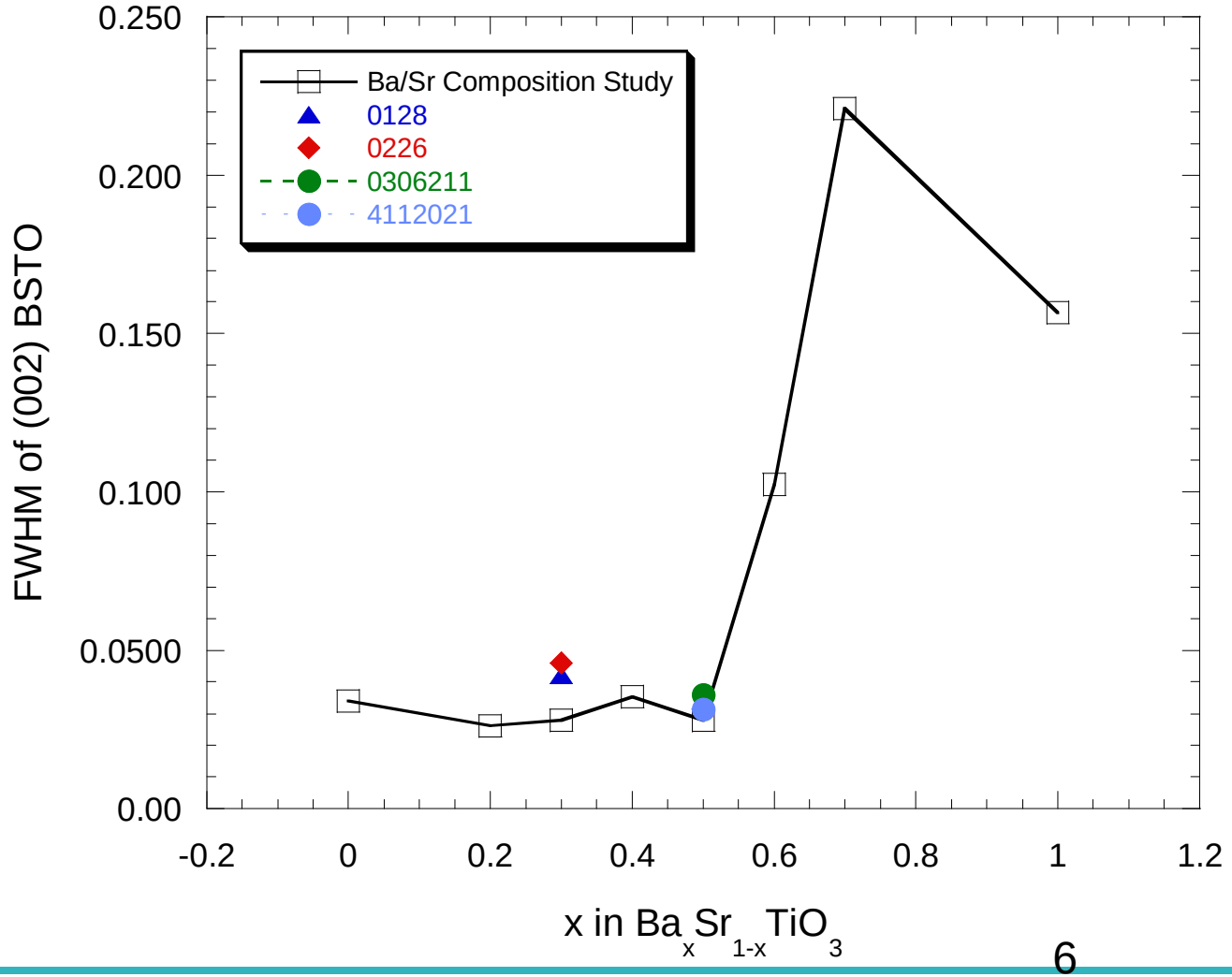

Coupled Microstripline Ferroelectric Phase Shifter in S_{21} Configuration

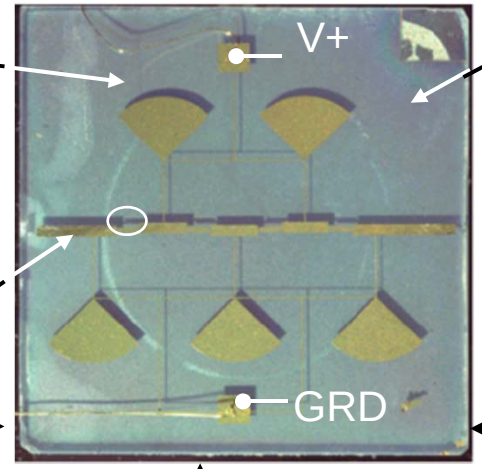

Radial Stub Bias Tee

Ferroelectric Phase Shifter Element (1 of 4)

Magnesium Oxide Substrate (500 μm Thick)

180 degrees total phase shift at 350 volts bias

1 cm

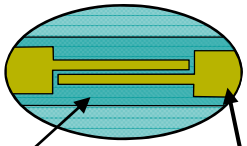

Cr-Au, 2μm

Laser Ablated Ba50Sr50TiO3 0.35 μm film

Phase shifters using paraelectric films on MgO substrates achieved ≈60°/dB insertion phase shift/loss.

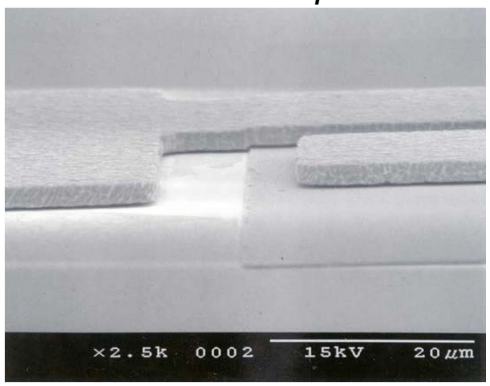

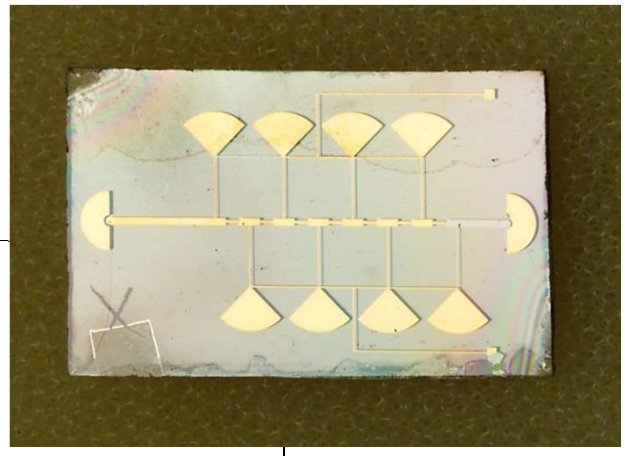

1.2 cm

0.3 mm MgO with a ≈400 nm Laser Ablated $Ba_xSr_{1-x}TiO_3$ Film "Probe-able" phase shifter

"K-Band Phased Array Antennas Based on $Ba_{60}Sr_{40}TiO_3$ Thin Film Phase Shifters, R. Romanofsky et al., IEEE Trans. MTT, Vol. 48, No. 12, pp. 2504-2510, 2000

X-Band Hybrid Ferroelectric/ Semiconductor Phase Shifter

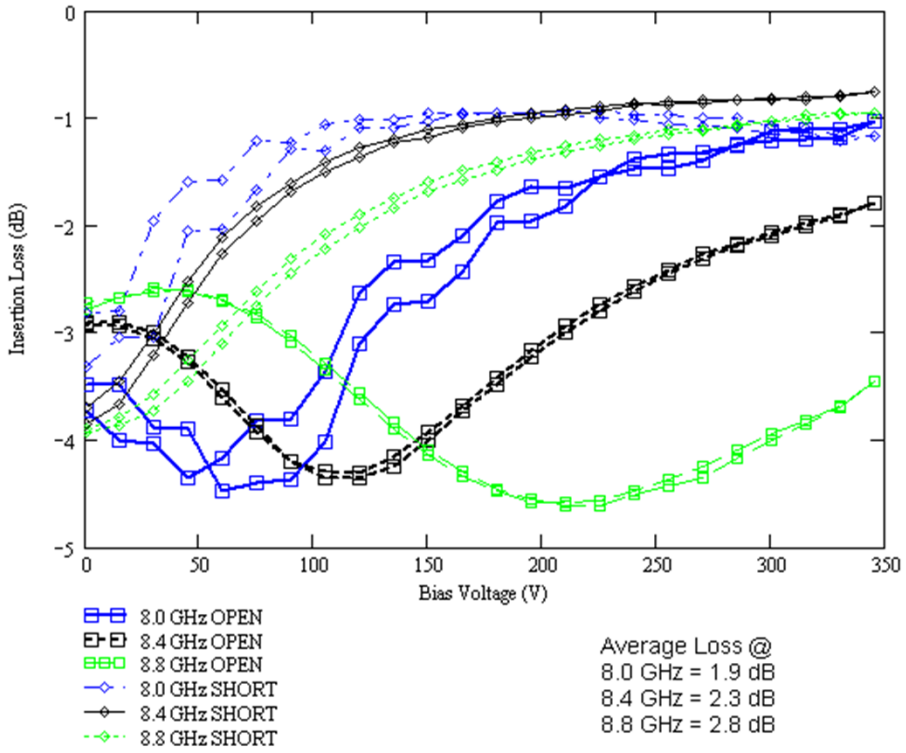

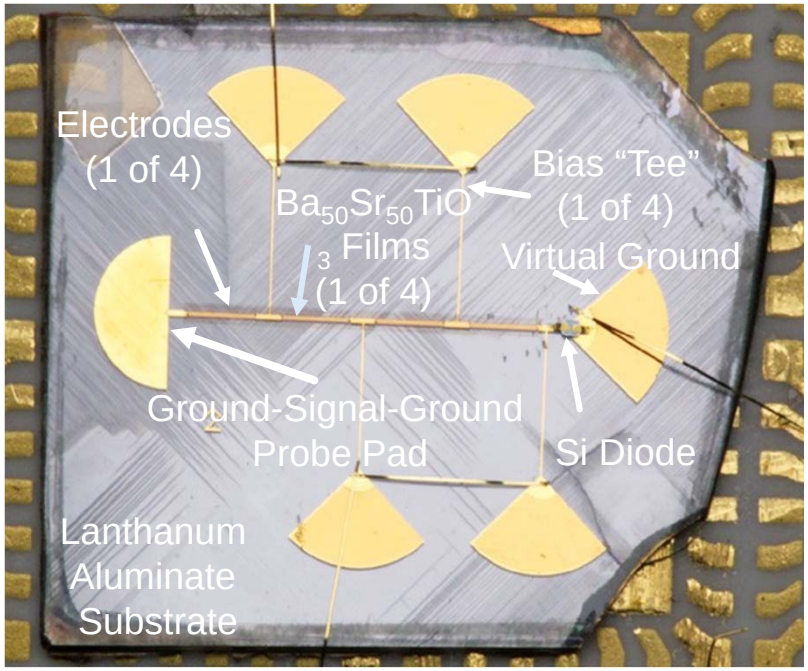

Photograph of prototype X-band phase shifter with 4 coupled microstripline sections and Si diode switch, which produced ≈310° of phase shift with 2.5 dB insertion loss.

EM Simulation of Hybrid X-band Phase Shifter

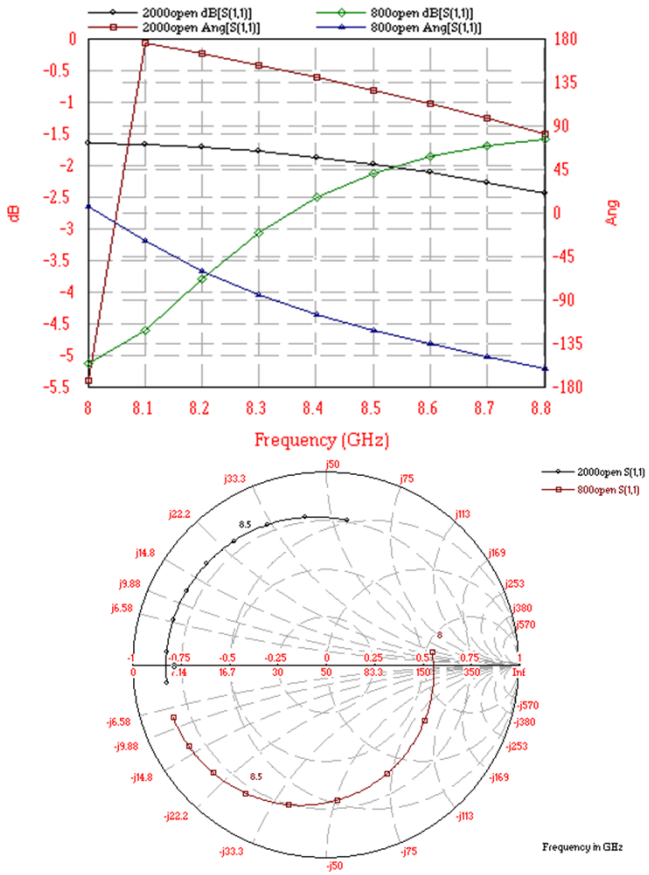

Insertion loss (Top - left axis) and insertion phase (Top -right axis) for SPST switch open and corresponding impedance data.
Average Loss=2.5 dB

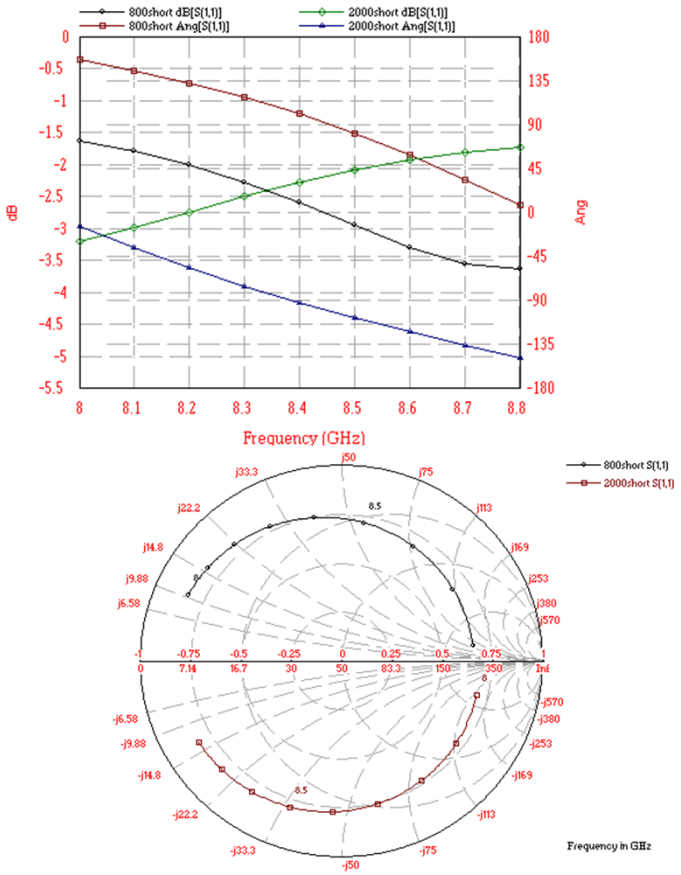

Insertion loss (Top - left axis) and insertion phase (Top - right axis) for SPST switch short and corresponding impedance data.
Average Loss=2.3 dB

Hybrid X-Band Ferroelectric Phase Shifter
Measured Results with Wire-Bond Switch

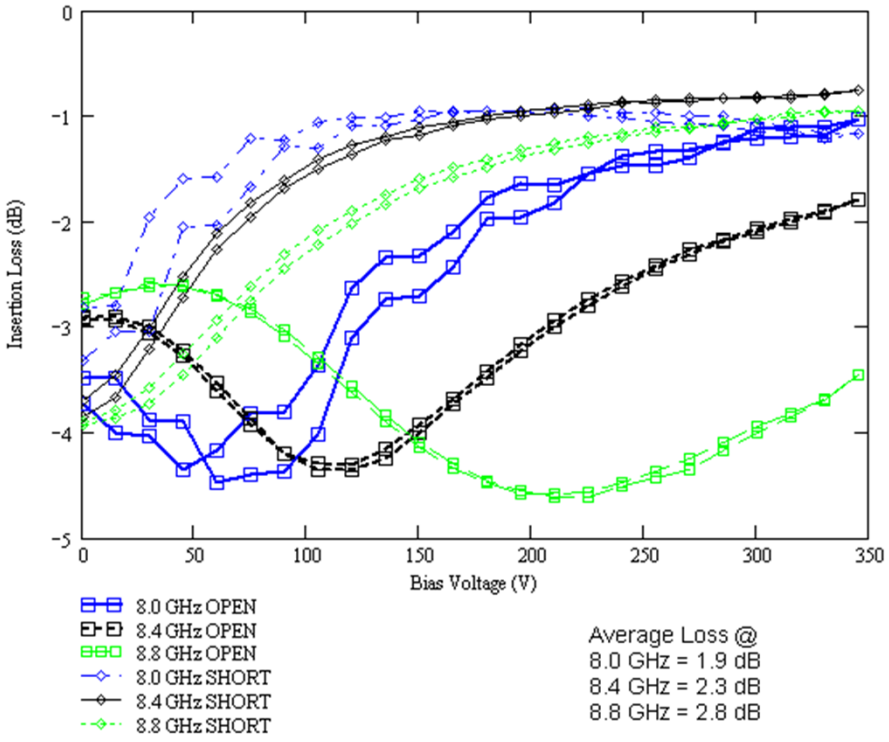

Average Loss @
8.0 GHz = 1.9 dB
8.4 GHz = 2.3 dB
8.8 GHz = 2.8 dB

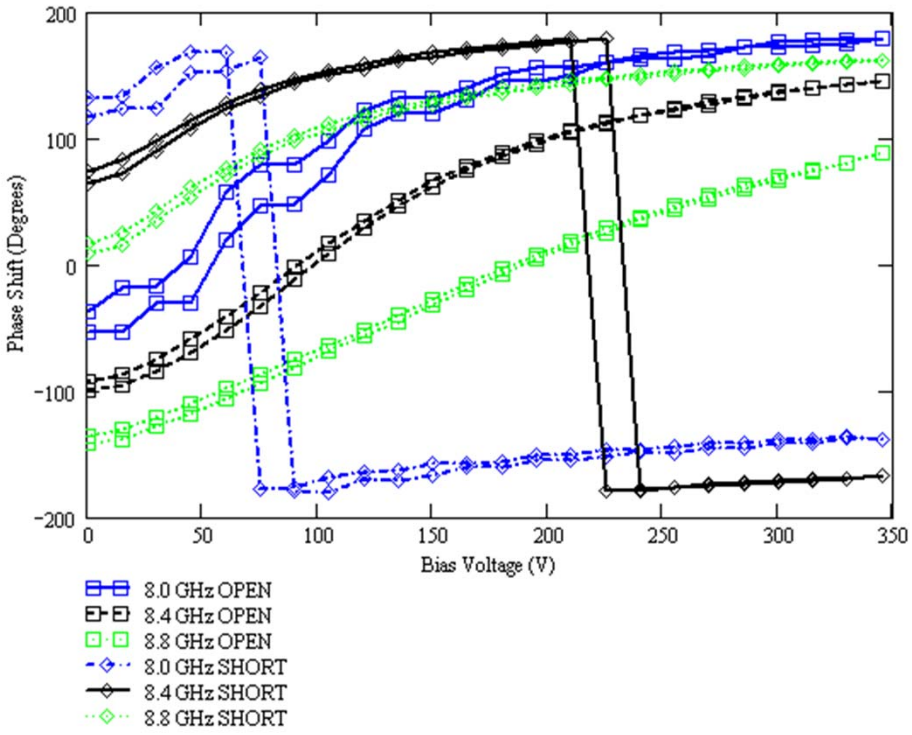

Hybrid X-Band Ferroelectric Phase Shifter Measured Results with Beam-Lead Si Diode Switch

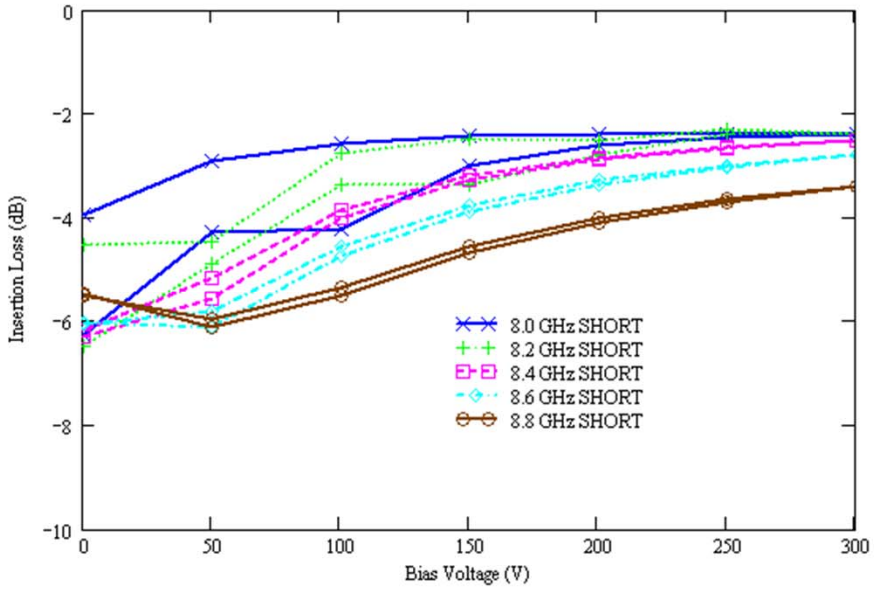

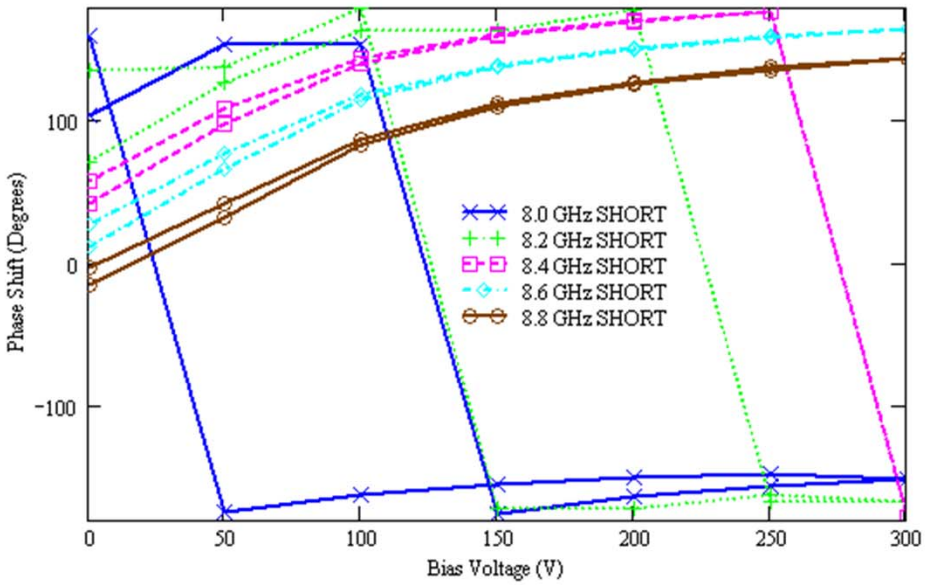

Diode “On”

Hybrid X-Band Ferroelectric Phase Shifter
Measured Results with Beam-Lead Si Diode Switch

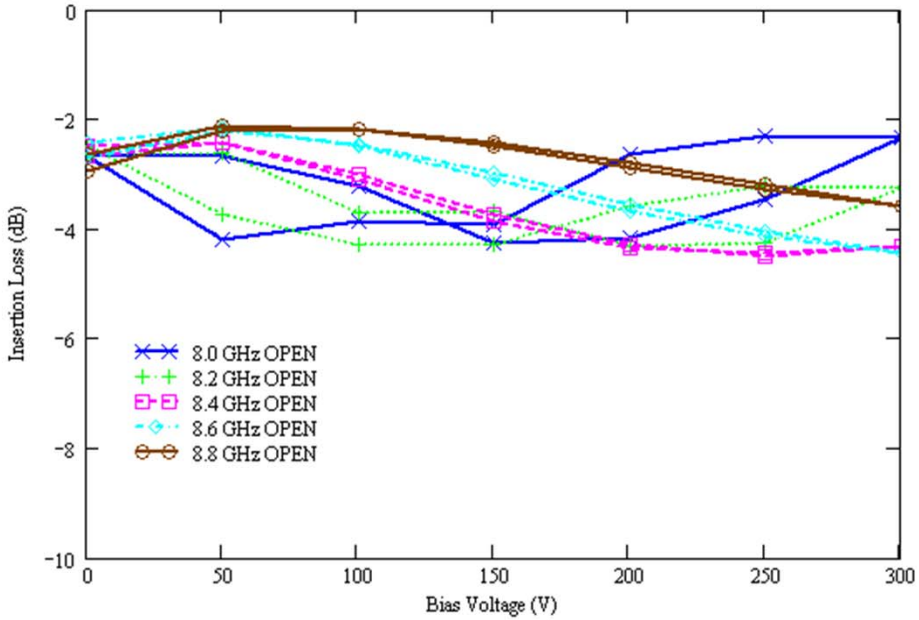

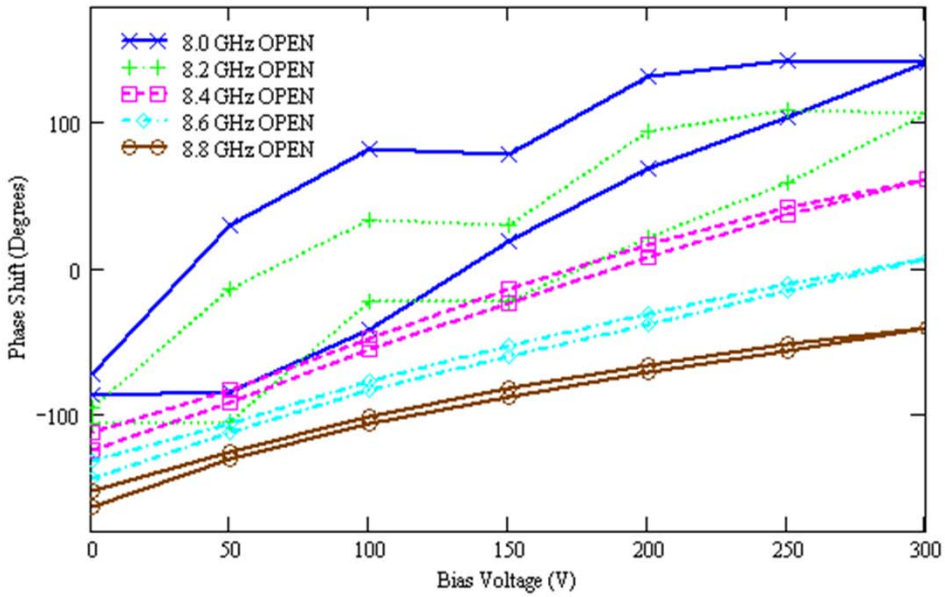

Diode “Off”

Typical Coupled Microstripline (Baseline) Ferroelectric Phase Shifter in Reflection Mode

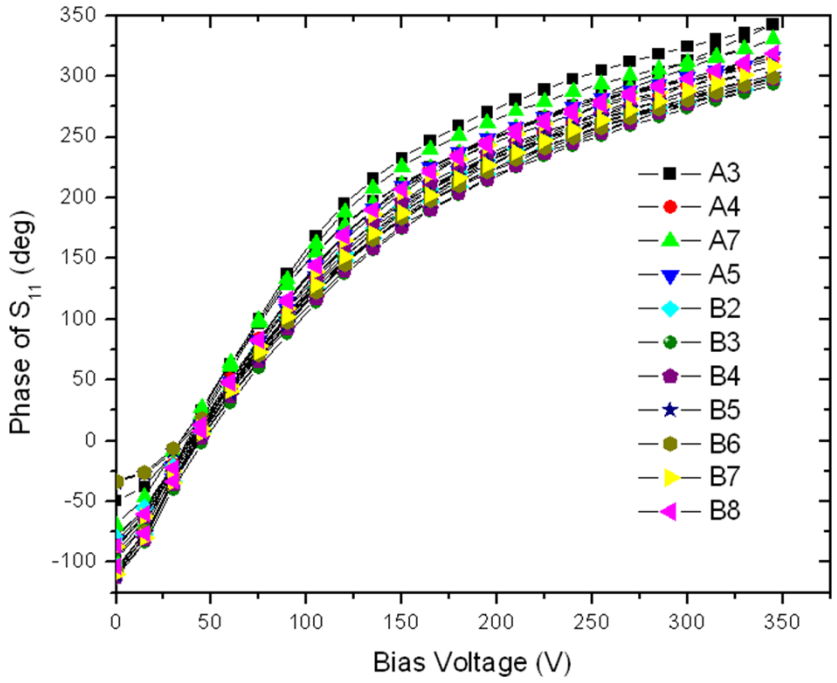

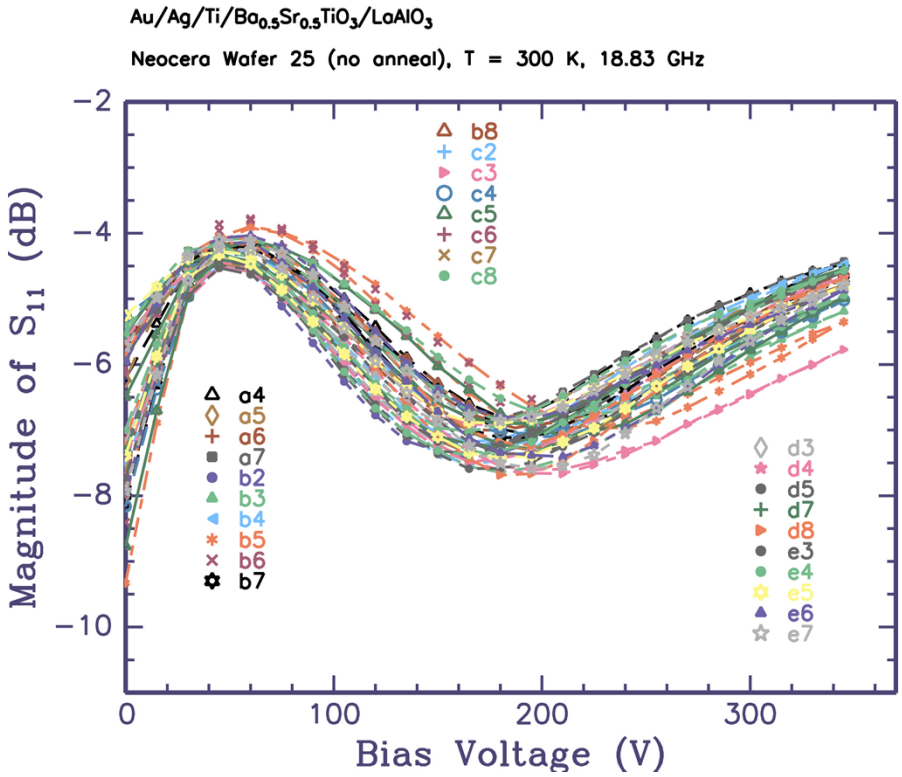

3 λ 25 Ω $Au/SrTiO_3/LaAlO_3$ Tunable Ring Resonator

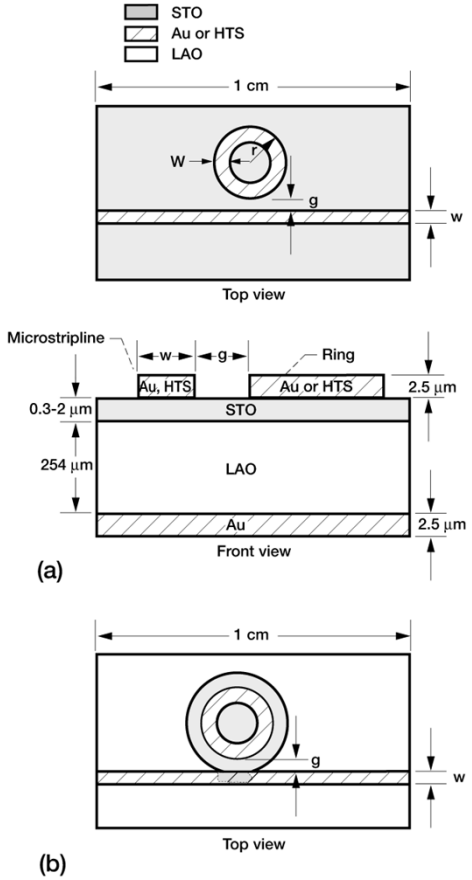

FIGURE 1 Microstripline side-coupled ring resonator. W = 406 μm for the 25 Ω ring and 89 μm for the 50 Ω ring. w = 89 μm and g = 25μm, r = 1694 μm.

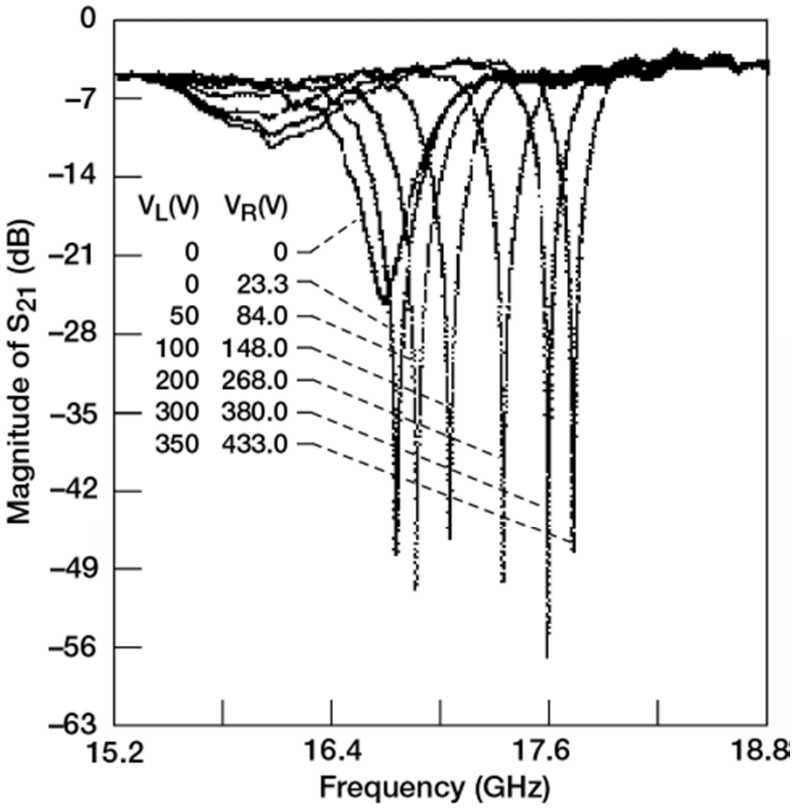

Figure 2.—$|S_{21}|$ of the side-coupled $Au/SrTiO_3/LaAlO_3$ resonator as a function of bias. The voltages correspond to the dc bias on the ring (V_R) and microstrip line (V_L).

Cryogenic GaAs PHEMT/Ferroelectric Ku-Band Tunable Oscillator

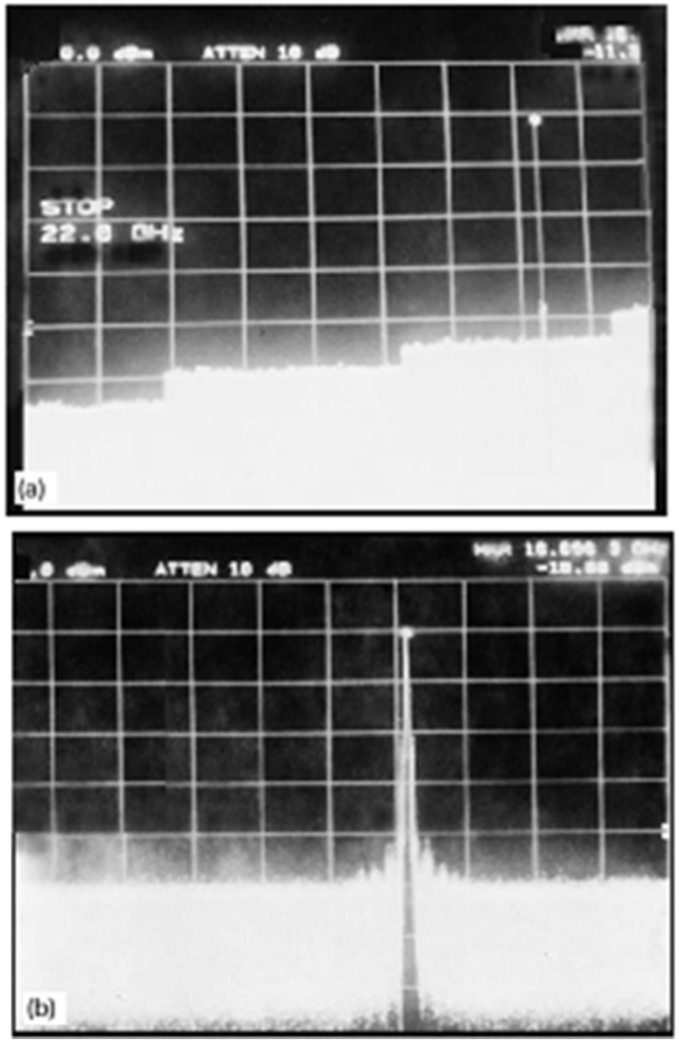

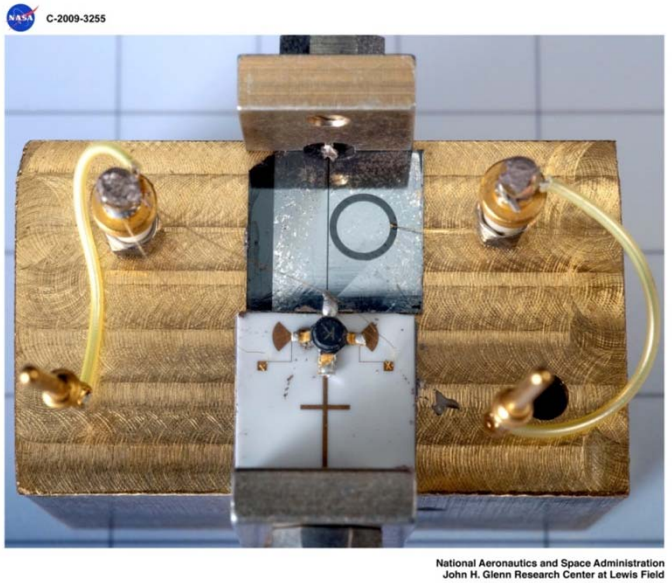

A Side-Coupled Au/$SrTiO_3$ 3λ Ring Resonator Provided Over 500 MHz Tuning at Ku-Band.
The Laser Ablated Ferroelectric Film was 2 μm Thick.
Bias was between 0 and 250 V.

"A Cryogenic GaAs PHEMT/Ferroelectric Ku-Band Tunable Oscillator," R.R. Romanofsky, F.W. VanKeuls, and F.A.Miranda, Journal De Physique IV, Vol. 8, 1998, pp. 171-174. (NASA TM-206967)

Reflectarray Concept

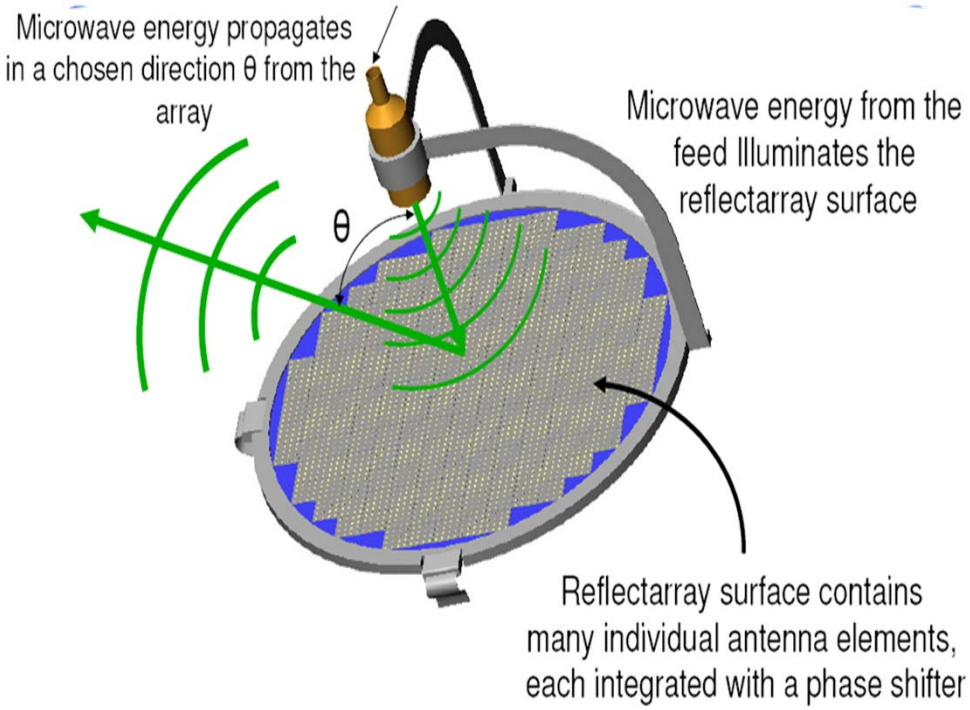

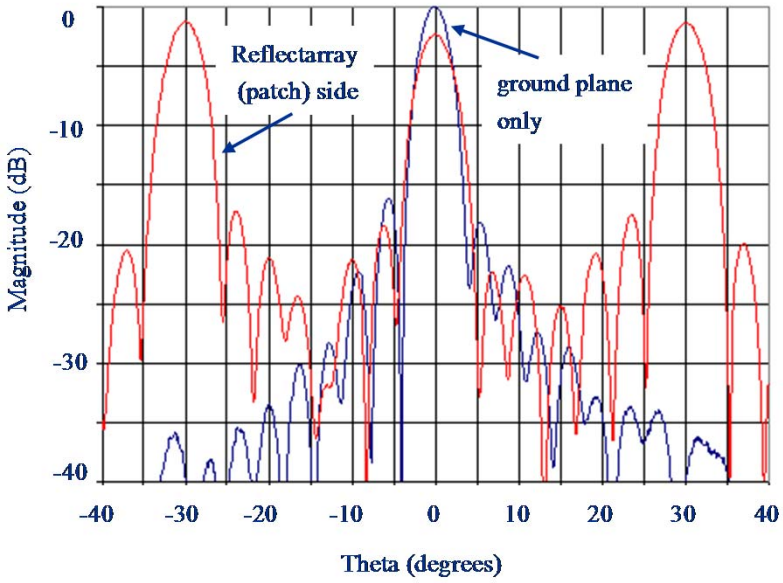

Measured 19 GHz radar cross section of a 208 element passive reflectarray constructed on 0.79 mm thick substrate with εr=2.2

615 Element K-band Reflectarray and Low Power Controller

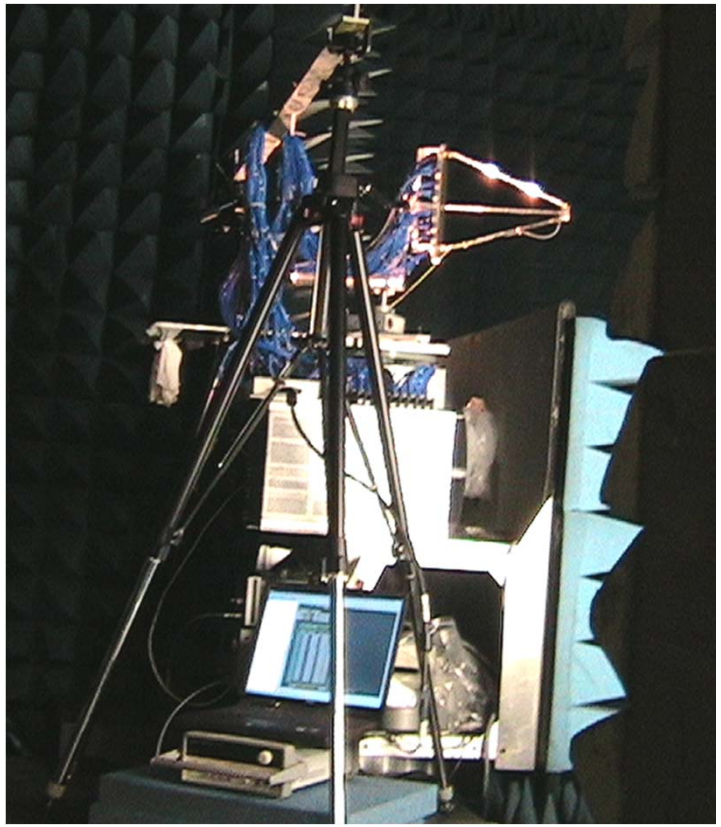

Prototype Ferroelectric Reflectarray, Custom Power Supply and Controller in GRC Far-Field Antenna Range

"Advances in Scanning Reflectarray Antennas Based on Thin Ferroelectric Film Phase Shifters," R. Romanofsky, Proc. IEEE, Special Issue on Technical Advances in Deep Space Communications and Tracking, Vol. 95, No. 10, Oct. 2007, pp. 1968-1975

Origin of ISI/BER Analysis

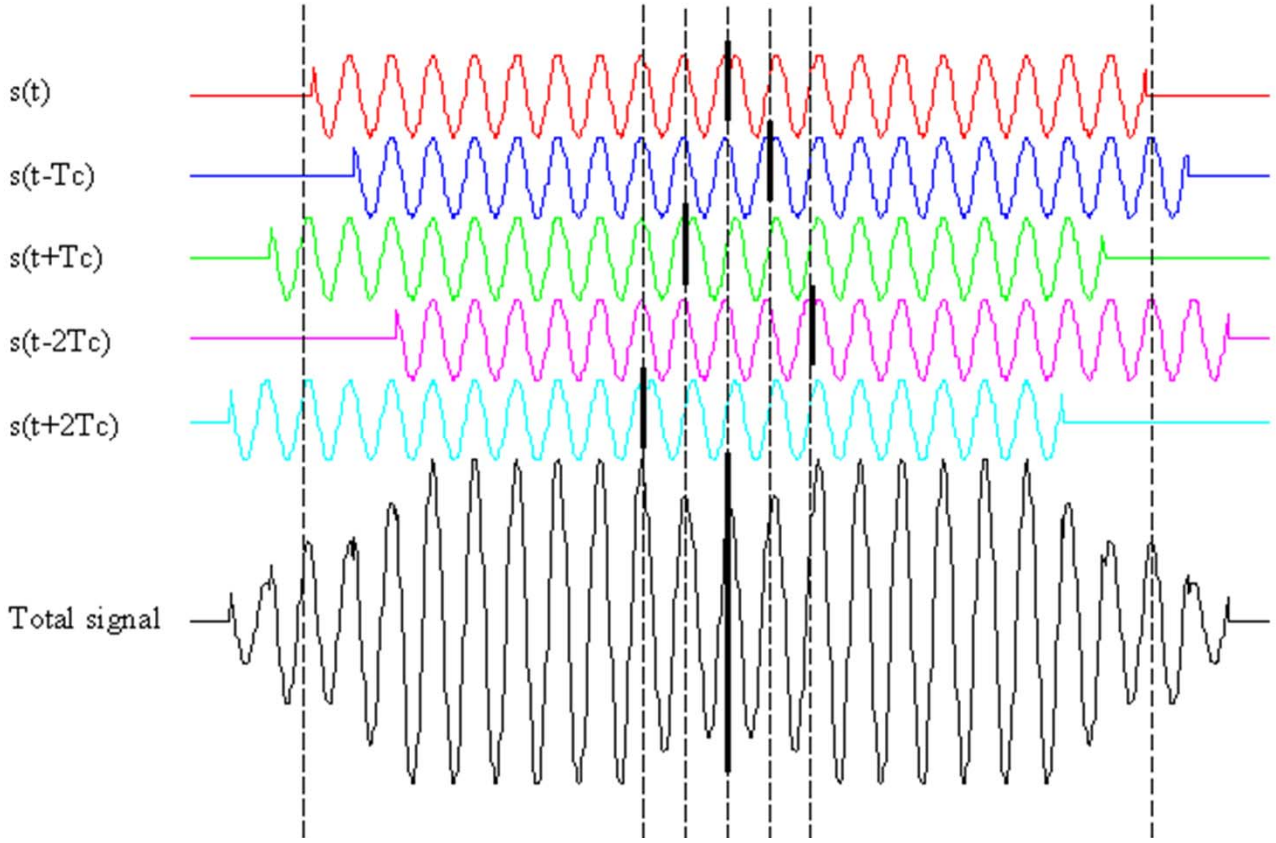

Formation of Inter-symbol Interference (ISI) due to Different Delays in Signal Components

"Study of Behavior of Digital Modulations for Beam Steerable Reflectarray Antennas," F. Xiong and R. Romanofsky, IEEE Trans. Ant. and Prop., vol. 53, No. 3, March, 2005, pp. 1083–1096

Effect of Phase Shifter Behavior on BER

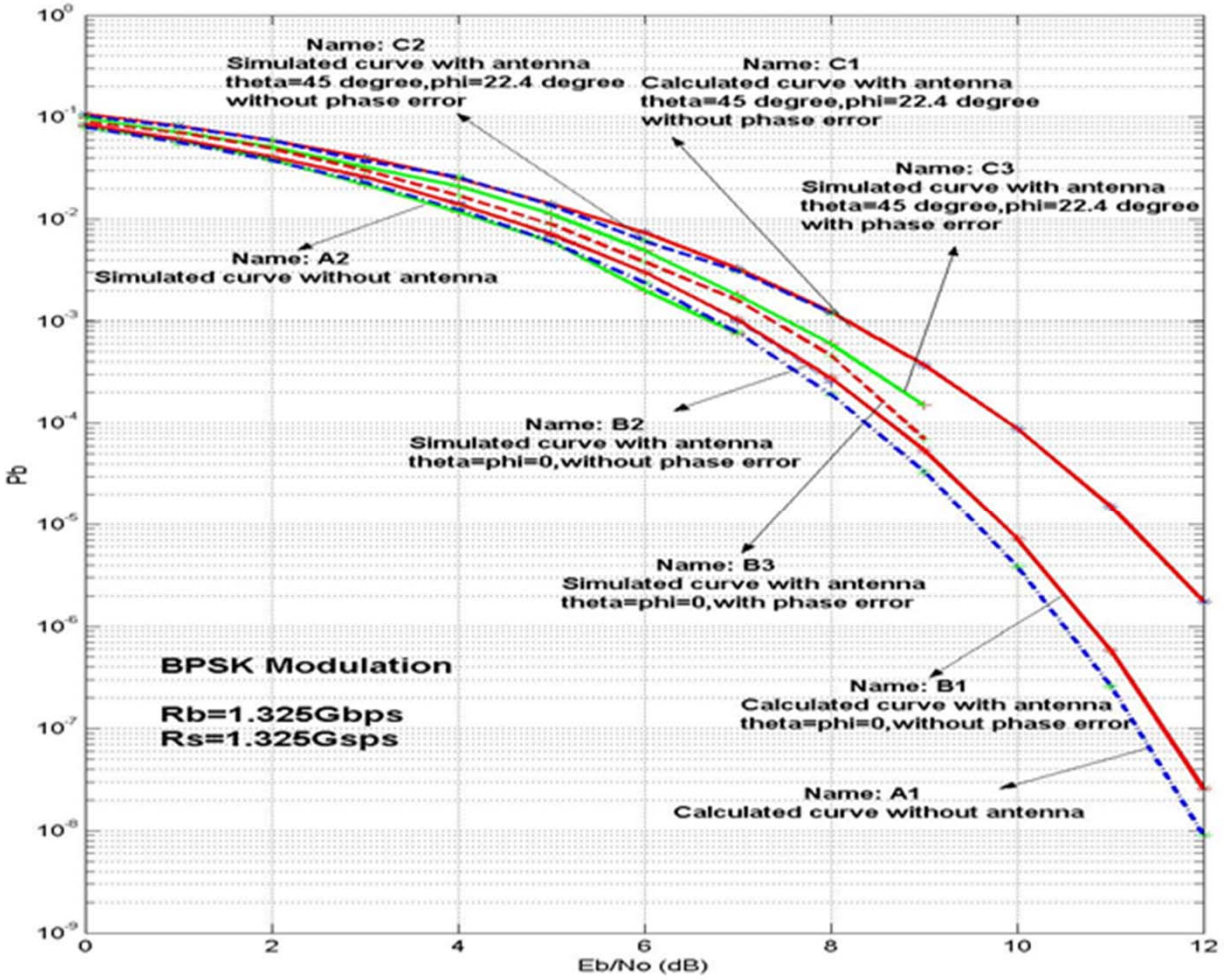

BER Curves of BPSK

Radiation Testing at the University of Indiana Cyclotron Facility

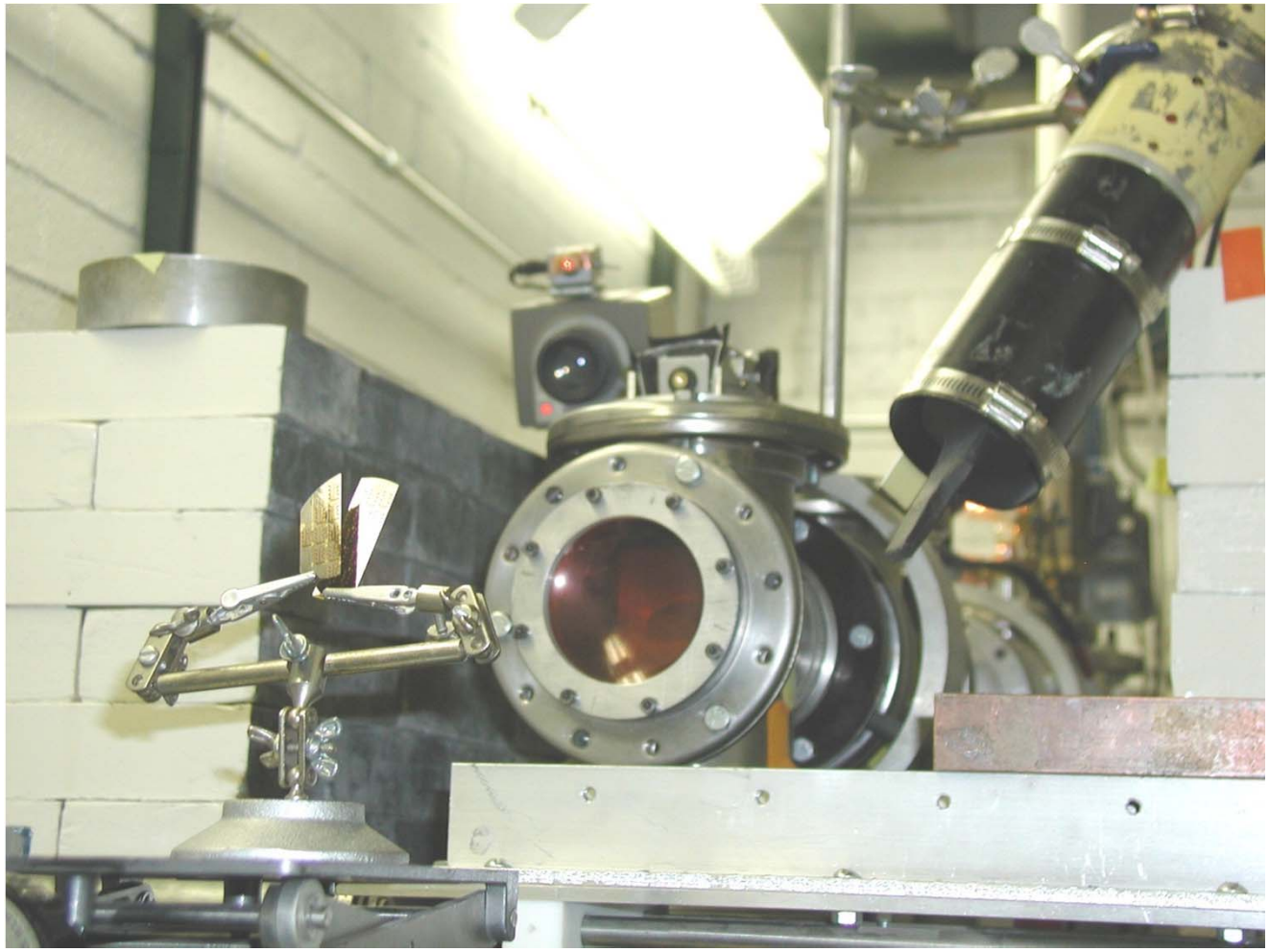

Total Dose Radiation Tests
Effect on Loss

Data @ 19 GHz, Wafer # 24

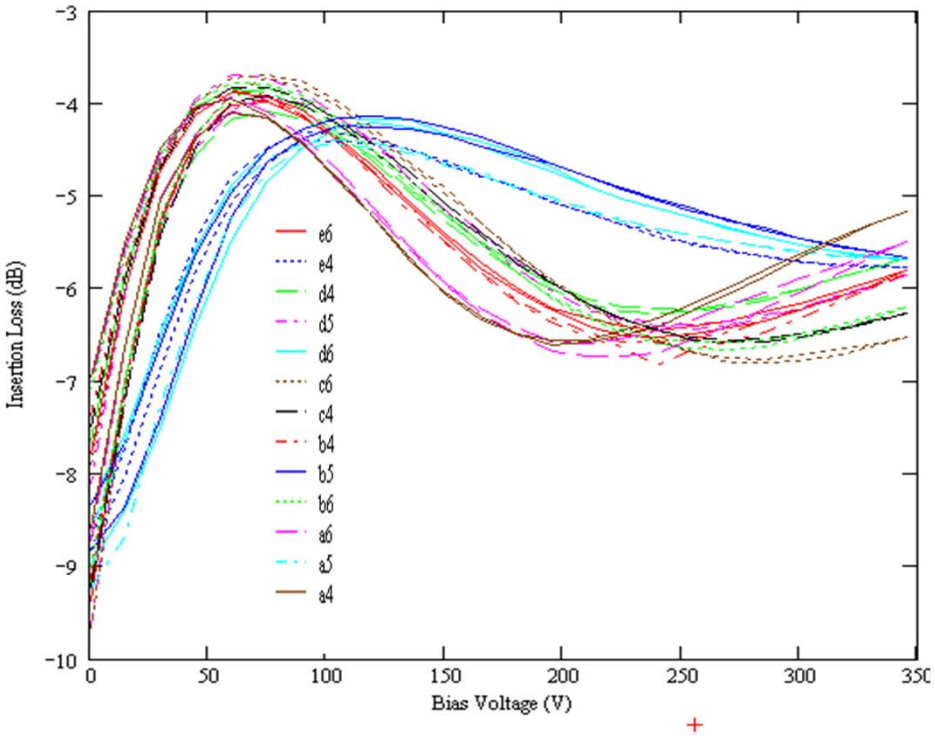

AVERAGE LOSS=5.58 dB

Average Loss @ 0 Field=8.46 dB

13 Pristine Devices from Wafer 24

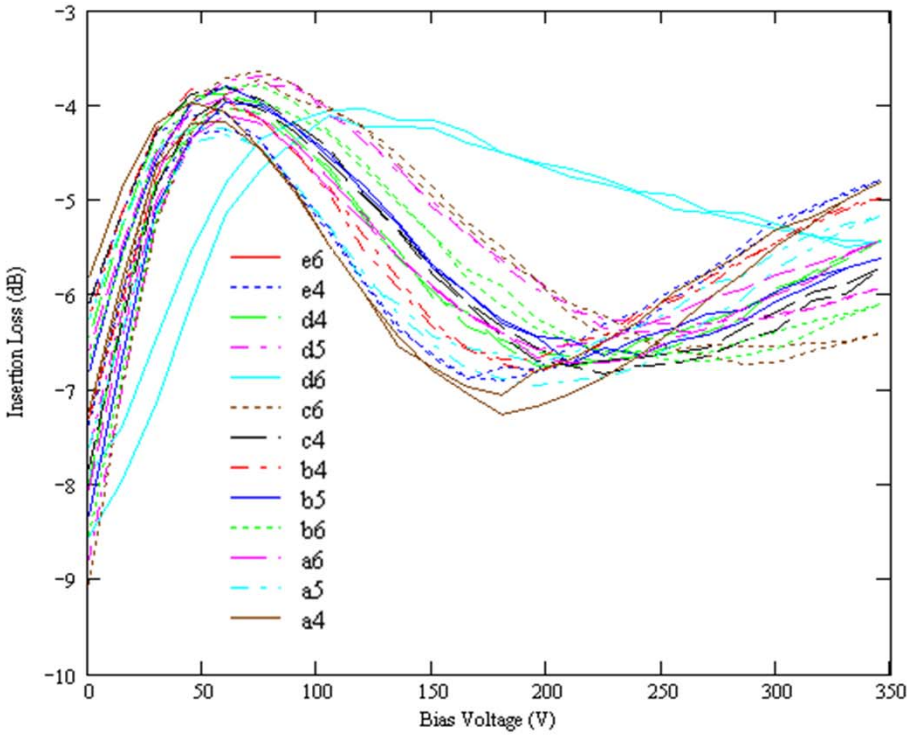

AVERAGE LOSS=5.62 dB

Average Loss @ 0 Field=7.47 dB

Same devices after exposure to 197 MeV protons (at target). Total fluence=$9.9486 \times 10^9/cm^2$ *

*Equivalent to 10 years in the International Space Station Hab Module

Total Dose Radiation Tests
Effect on Phase

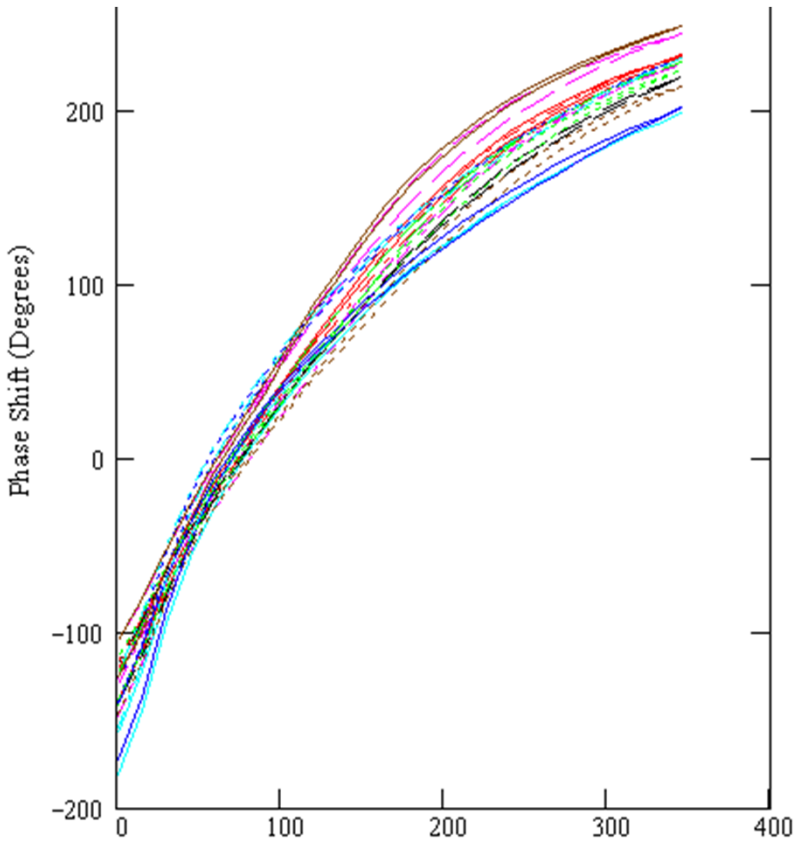

Bias Voltage (V)

13 Pristine Devices from Wafer 24

*Equivalent to 10 years in the International Space Station Hab Module

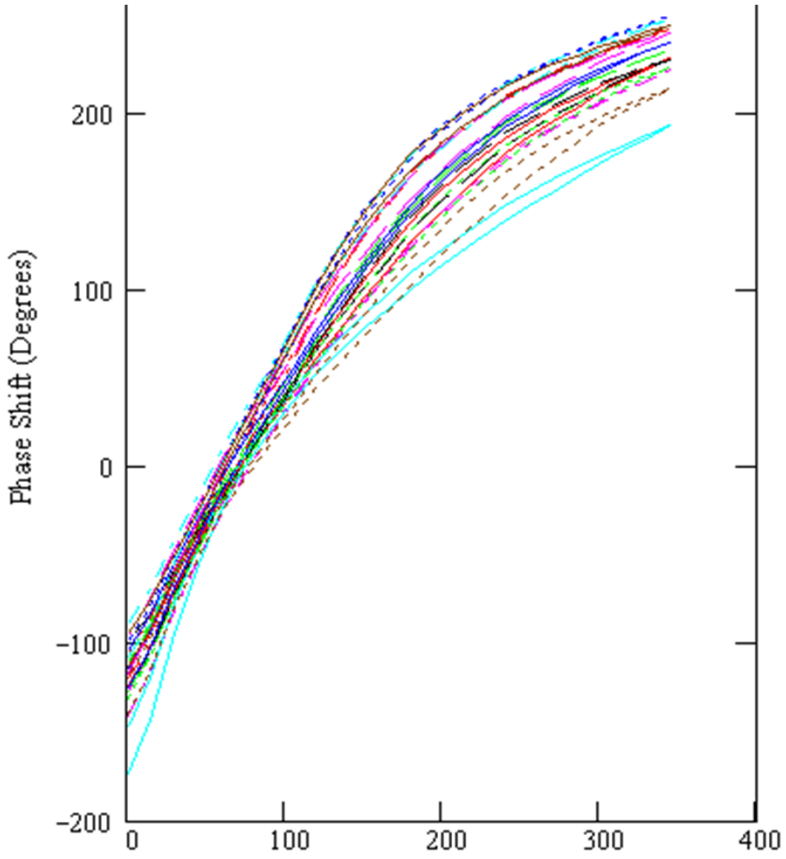

Bias Voltage (V)

Same devices after exposure to 197 MeV protons (at target). Total fluence=$9.9486 \times 10^9/cm^2$ *

Flight Validation Rationale: Fundamental change in scanning array design, materials and fabrication requires flight validation to demonstrate space flight worthiness.

Experiment Objective

The objective of the "reflectarray" experiment package is to characterize performance of critical components associated with the reflectarray antenna system as a prelude to a fully functional reflectarray space experiment. The operational scenario of MISSE-8, assuming a nadir facing ExPA mount, is similar to an operational scenario involving direct downlink from a LEO spacecraft.

1. Evaluate performance of FPGA 128 channel based high-voltage controller board. Rad Hard FPGA available from Actel. Supertex amplifiers/sample & hold are COTS.

2. Characterize on-orbit performance of phase shifters based on thin "ferroelectric" films. Evaluate effect of temperature cycling and long term effects of LEO radiation and AO, etc. exposure.

3. Employ lessons learned to develop a complete reflectarray antenna system and plan space experiment follow-on to execute actual communications link..

Ferroelectric Reflectarray Critical Components Experiment Flight Hardware Concept

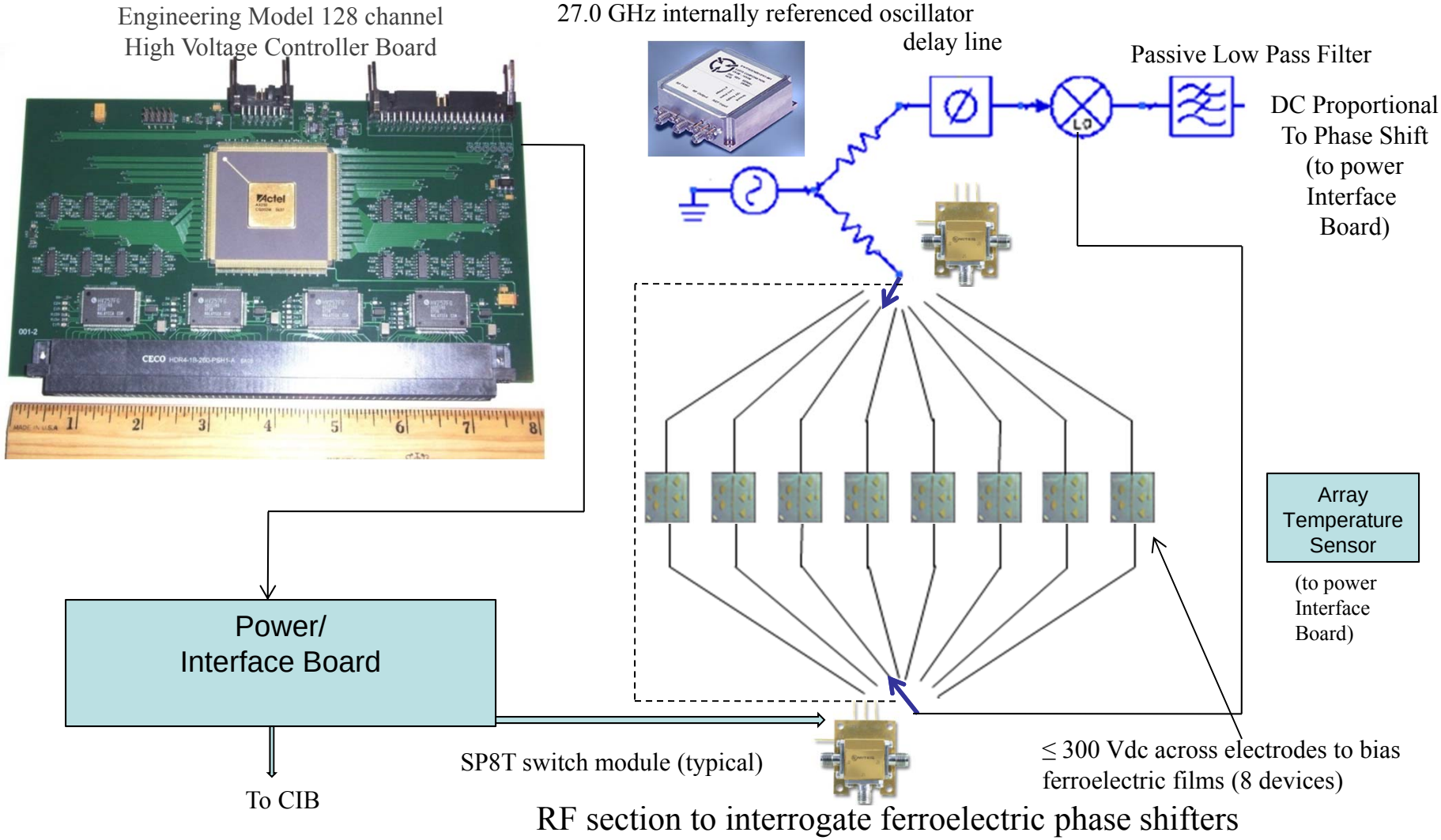

RF section to interrogate ferroelectric phase shifters

Ferroelectric Reflectarray Critical Components Experiment (F-Recce)

Delivered “Ferroelectric Reflectarray Critical Components” MISSE-8 experiment hardware to NRL (overall system integrator) in February, 2010

Experiment Objective:

•To characterize long duration on-orbit performance of critical components of a reflectarray antenna system as a prelude to a fully functional reflectarray space experiment.
• Set the stage for a follow on science experiment to investigate the relationship between 1/f noise and gravity

Reflectarray Benefits:

•Combines best features of a gimbaled dish and a phased array
  •Dishes pose reliability risks (e.g. dust exposure) and limited slew rates
  •Phase arrays are expensive and inefficient
•10-100x cost reduction to phased array
•Low power
•Large aperture size (not gain limited)
•Cooling not an issue
•High reliability- no moving parts
•Reciprocal surface- transmit & receive on same surface

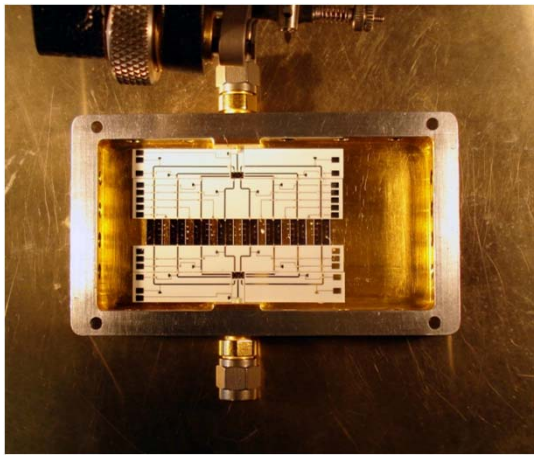

RF Module

Flight:

STS-134, Endeavor, May 16,2011

PI:

RHA/Dr. Robert Romanofsky

Team: L. McQuaid, N. Varaljay, D. Raible, F. Van Keuls, D. Priebe, E. Sechkar, N. Adams

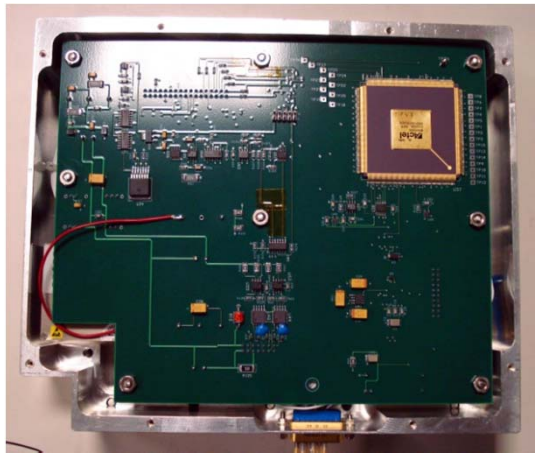

Experiment tray with Power/Interface/Control board (top) and RF Electronics board (bottom) installed.

ISS Radiation Environment

- ISS environment is suitable for an SEE experiment
  - High inclination (51.5º) exposes ISS to higher fluences of trapped electrons and protons and solar and galactic cosmic rays than would be the case in a lower inclination orbit with the same altitude range, largely as a result of the overall shape and magnitude of the geomagnetic field
  - ISS passes through the South Atlantic Anomaly (SAA)

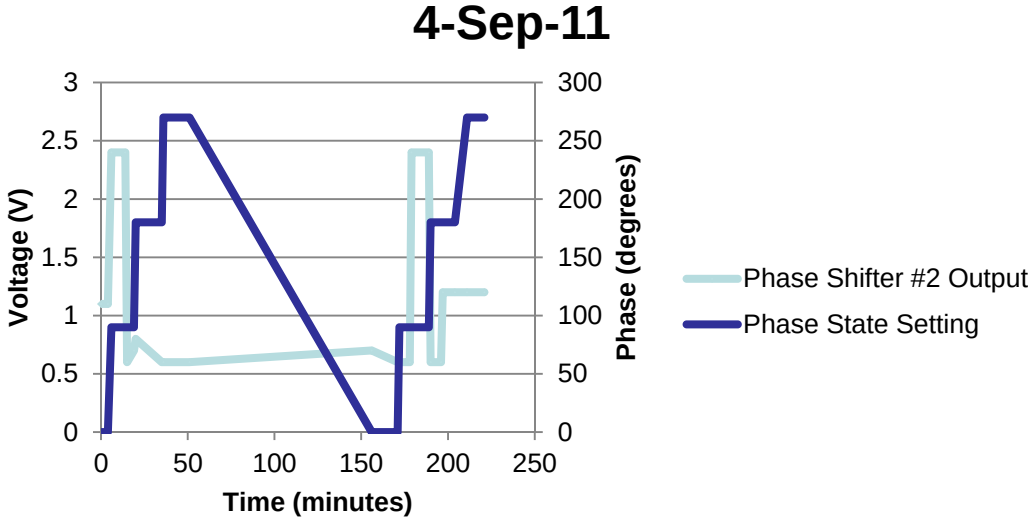

Typical performance telemetry

Ferroelectric Reflectarray Critical Components Experiment (F-Recce)

Mission Specialist Drew Feustel with MISSE-8 on the outside of the International Space Station. *Photo credit: NASA*

F-Recce was developed by NASA's Glenn Research Center in Cleveland, Ohio, to accelerate mission insertion opportunities for a new type of " phased-array" antenna - an antenna that can redirect its main beam without physically repositioning itself. Conventional parabolic reflectors require a sophisticated mechanized gimbal system to steer the beam. This can be a prohibitively slow process plus all mechanical systems in space potentially suffer reliability problems because of the harsh environment. F-Recce will characterize critical components associated with NASA Glenn's reflectarray antenna system, including NASA Glenn invented thin film ferroelectric phase shifters, as a prelude to a fully functional space demonstration in a Low Earth Orbiting environment. Applications include: inter-satellite communications links, space-based radar/precipitation radar, docking and rendezvous, landing terrain radar, automotive collision avoidance radar, and others. The conditions of space are harsh and it is not easy to reproduce the combined environments to measure the effects of particle radiation, atomic oxygen, thermal cycling and ultraviolet conditions in labs.

Reflectarray Power Supply

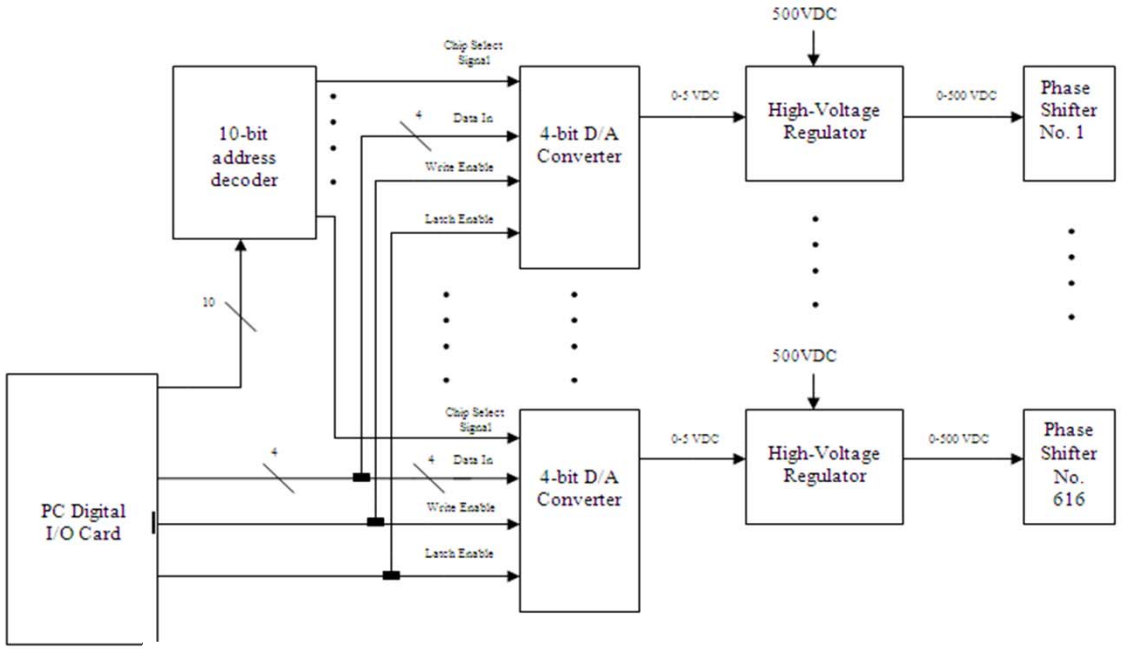

Multilayer Piezoelectric Transformer

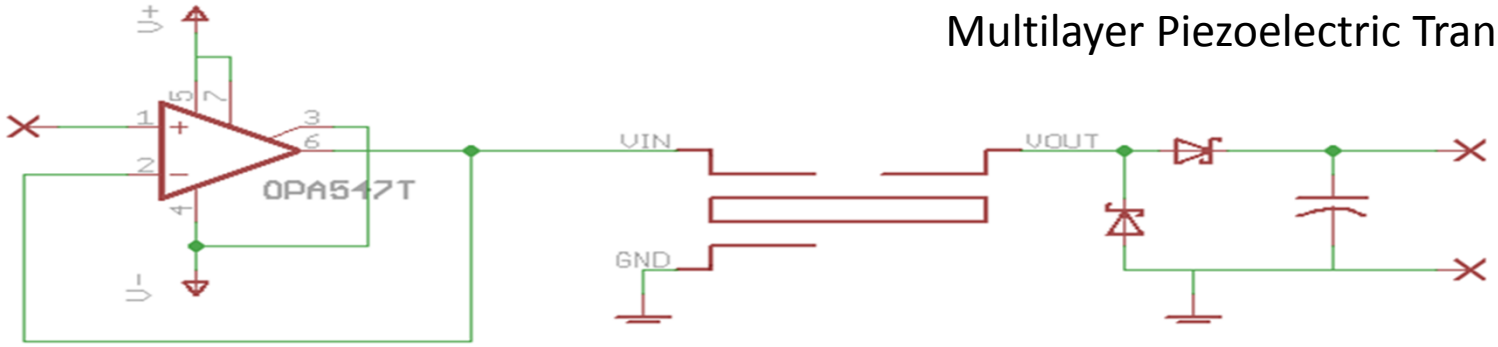

Proof-of-Concept Driver Circuit

Explore the Potential of a Piezoelectric Transformer as a Replacement for the Magnetic Transformer in an AC/DC Converter to Drive Ferroelectric Phase Shifters

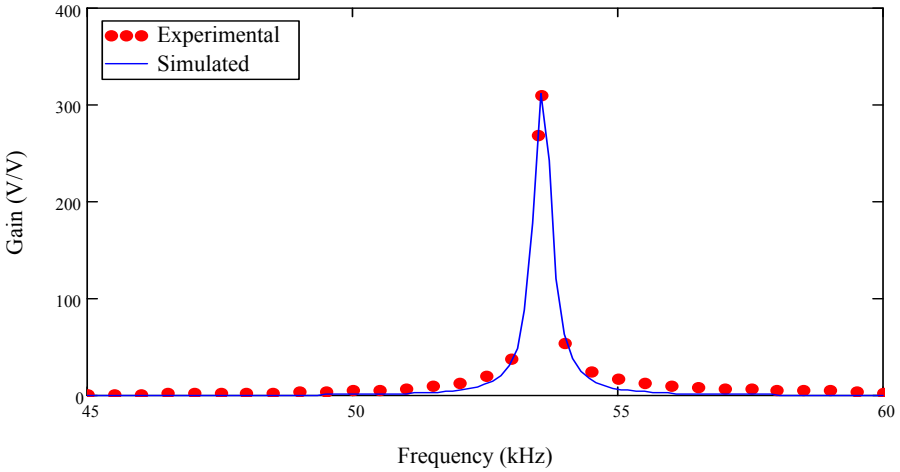

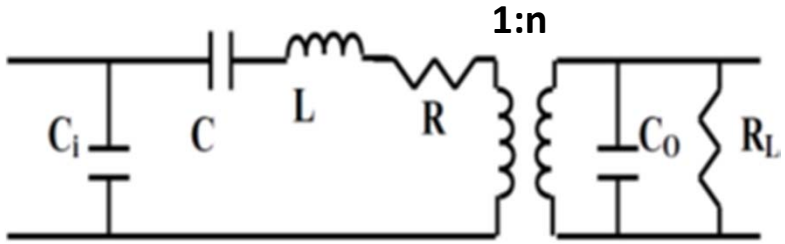

$$\frac{Vo}{Vi} = \frac{sR_LC}{s^3n^2R_LC_OLC + s^2(n^2R_LC_OCR + n^2LC) + s(n^2R_LC_O + n^2CR + CR_L) + n^2}$$

The piezoelectric transformer is a high-Q system and is frequency, temperature, and load dependent

Two approaches to driving the circuit were used: the first was fixing the drive frequency at the resonant frequency of 54.7 kHz and varying the input to achieve desired output voltages, and the second was fixing the input voltage to the minimum necessary for reaching the 300 VDC and sweeping the frequency.

"Implementing a Piezoelectric Transformer for a Ferroelectric Phase Shifter Circuit," A. Roberts and R. Romanofsky, *Integrated Ferroelectrics*, 134:102–110, 2012

Cross Sectional TEM of a heterostructure consisting of 80 nm $(ZrO_2)_{0.91}(Y_2O_3)_{0.09}$/200 nm $Bi_4Ti_3O_{12}$/375 nm $Ba_{0.6}Sr_{0.4}TiO_3$ films on 100 Si

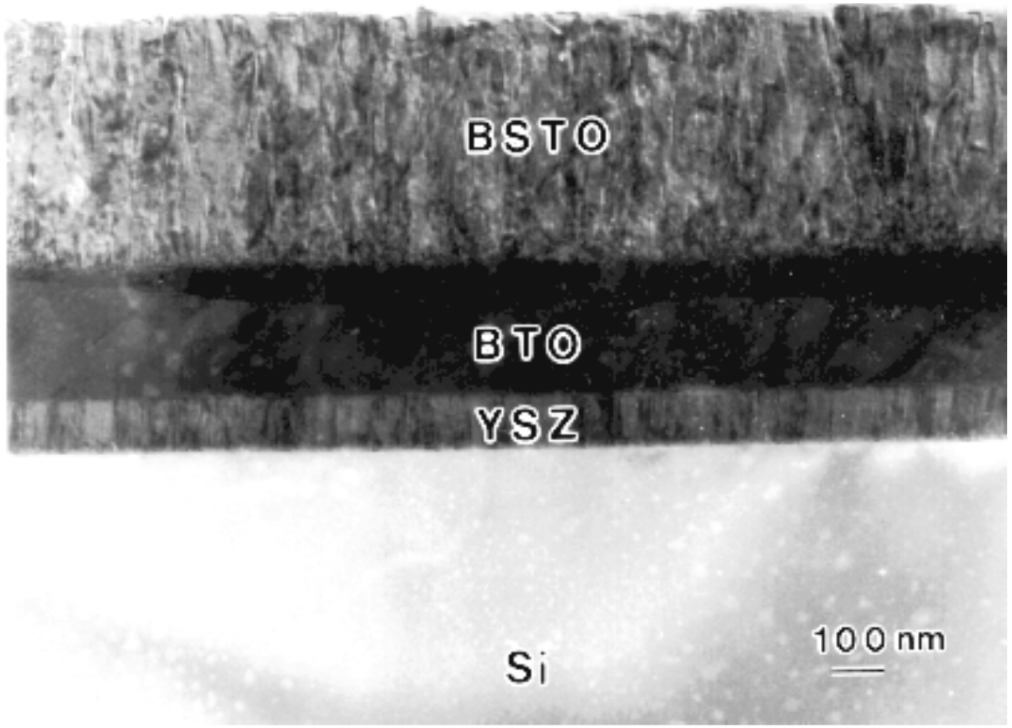

A thin interfacial layer is present at the YSZ-BTO interface. The BTO-BSTO interface appears abrupt.

Measured Reflection Coefficient of $Ba_{50}Sr_{50}TiO_3$/Si Patch

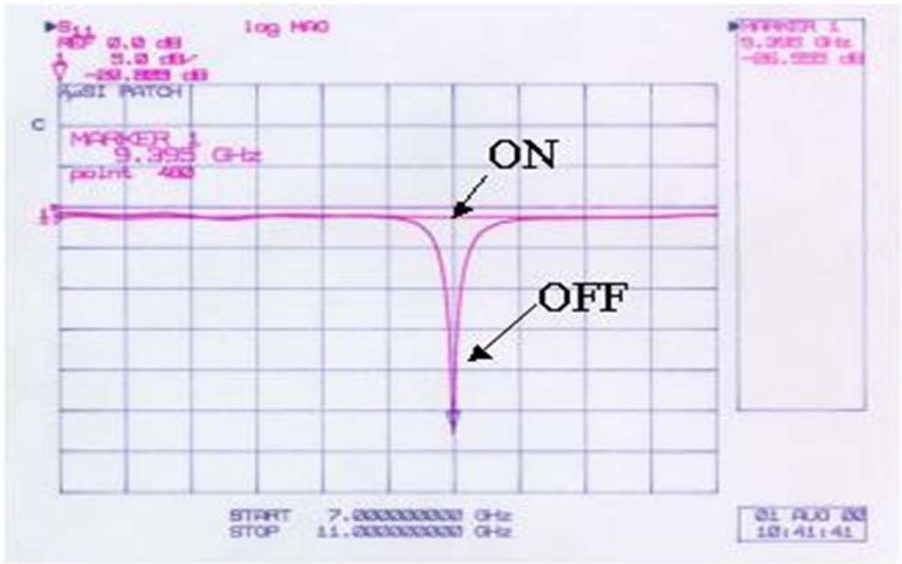

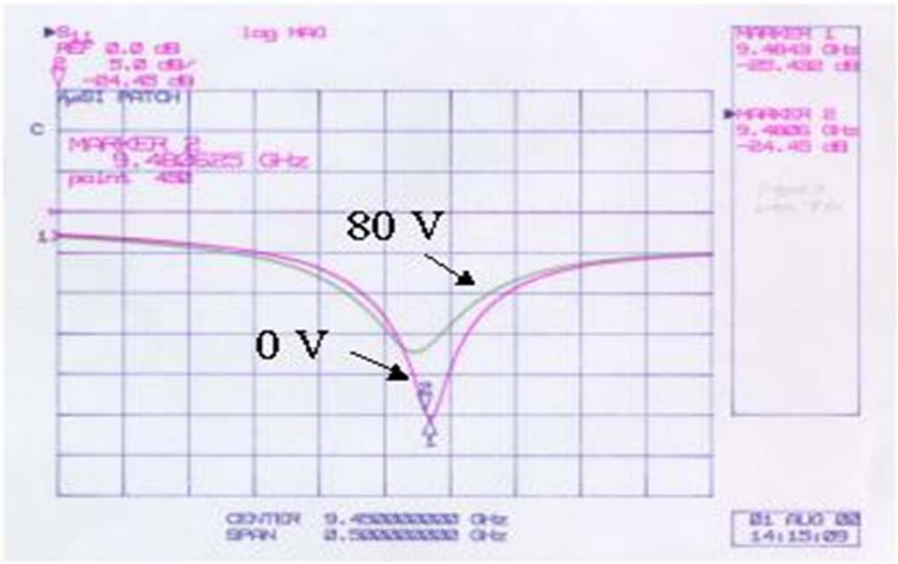

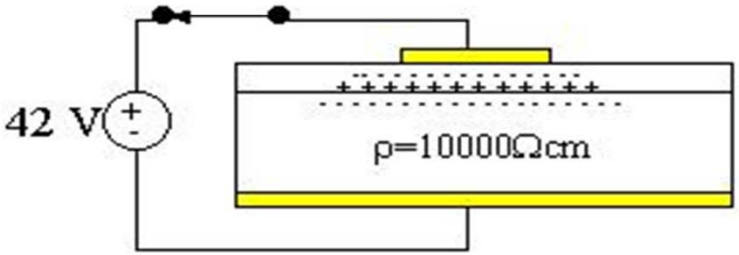

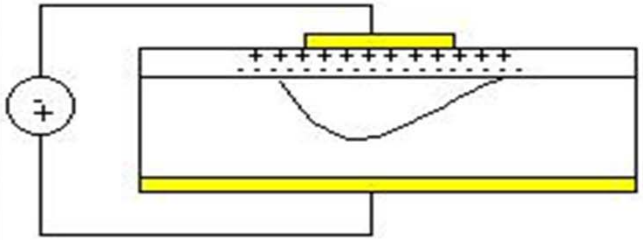

1/f Noise in Thin Ferroelectric Films

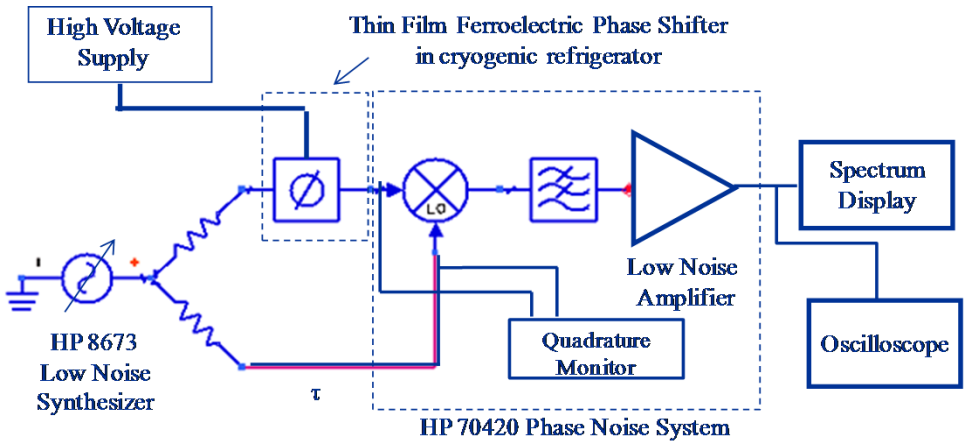

Residual cryogenic phase noise measurement system. The HP 70420 system contains the phase detector electronics and quadrature was achieved by slightly detuning the synthesizer frequency.

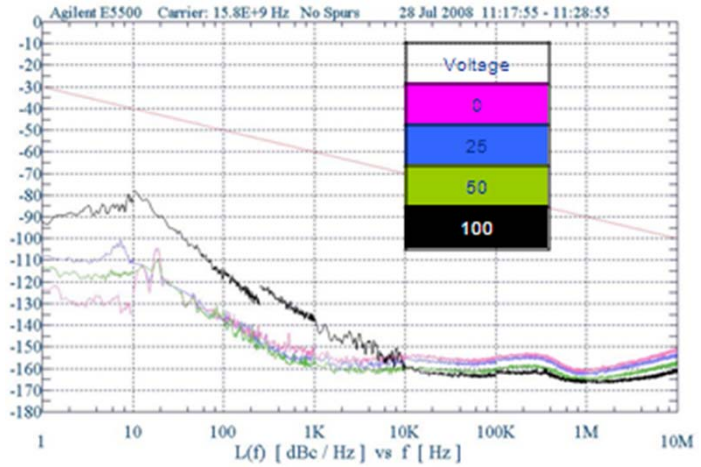

Phase noise profile of a nominally 350 nm $Ba_{0.5}Sr_{0.5}TiO_3$ film with a 15.8 GHz carrier at *T=290 K*. Bias across the interdigital structure is varied from 0 to 100 V in steps of 25 V

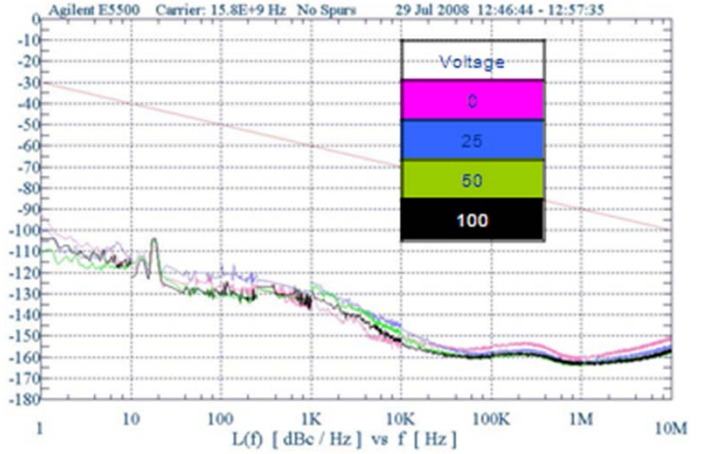

Phase noise profile of a nominally 350 nm $Ba_{0.5}Sr_{0.5}TiO_3$ film with a 15.8 GHz carrier at *T=140 K*. Bias across the interdigital structure is varied from 0 to 100 V in steps of 25 V.

Possible Magnetoresistive Effect from $Bi_4Ti_3O_{12}$/375 nm $Ba_{0.6}Sr_{0.4}TiO_3$ films on (001) Si (Sample Arranged in a van der Pauw Configuration)

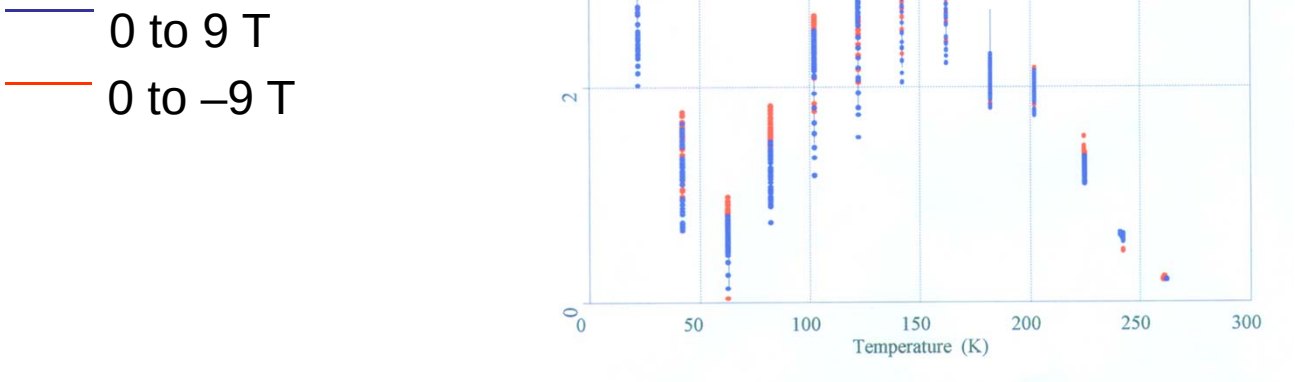

Conclusions

- Tunable microwave components, based on thin ferroelectric films, have been developed that rival the performance of, or even outperform, their semiconductor counterparts
- $Ba_xSr_{1-x}TiO_3$ films appear to be robust enough for space applications
- Thin ferroelectric film technology may enable new types of agile microwave components
- Low loss phase shifters based on ferroelectric films may enable new types of phased array antenna architectures
- The magnetoelectric effect – the induction of polarization by a magnetic field – was first postulated by Curie in 1894. Further evidence was presented here.
- Applications of ferroelectric films on semiconductor substrates is a largely unexplored area
- $Ba_xSr_{1-x}TiO_3$ is one of hundreds of potentially superior perovskite and non-perovskite based ferroelectric materials yet to be explored